Front. Energy Power Eng. China 2009, 3(2): 123–133
DOI 10.1007/s11708-009-0033-x

RESEARCH ARTICLE

Jason BASSI, Mark STRINGER, Bob MILES, Yang ZHANG

Terahertz time-domain spectroscopy of high-pressure flames

Abstract Laser spectroscopy in the visible and near infrared is widely used as a diagnostic tool for combustion devices, but this approach is difficult at high pressures within a sooty flame itself. High soot concentrations render flames opaque to visible light, but they remain transparent to far-infrared or terahertz (THz) radiation. The first far-infrared absorption spectra, to the best of our knowledge, of sooty, non-premixed, ethylene high-pressure flames covering the region of 0.2–2.5 THz is presented. A specially designed high-pressure burner which is optically accessible to THz radiation has been built allowing flame transmission measurements up to pressures of 1.6 MPa. Calculations of the theoretical combustion species absorption spectra in the 0.2–3 THz range have shown that almost all the observable features arise from H_2O. A few OH (1.84 and 2.51 THz), CH (2.58 THz), and NH_3 (1.77 and 2.95 THz) absorption lines are also observable in principle. A large number of H_2O absorption lines are observed in the ground vibrational in a laminar non-premixed, sooty flame (ethylene) at pressures up to 1.6 MPa.

Keywords terahertz time-domain spectroscopy, high-pressure flames, H_2O absorption lines

1 Introduction

The current understanding of combustion is based on atmospheric and low-pressure conditions, which are mostly bench-top configurations. Modern combustion systems, however, have to operate at high pressures. To further our understanding and development of such practical applications, a thorough investigation of combustion phenomena under actual operating conditions is of critical importance. High soot levels and pressures pose substantial challenges for current laser-based diagnostics, which operate in wavelengths from ultraviolet to near infrared. Most laser-based techniques were developed for cleaner flames.

Heavily sooted flames such as those found in jet engine combustors are difficult to study using laser-based diagnostics. At high pressure, the carbon (soot) particles are so dense that the flame is opaque to electromagnetic waves in the visible or near infrared. It has been found that a laser beam cannot probe the combustion field of a jet engine combustor even when the test pressure is below 1.0 MPa. Even when soot is not present, other obstacles such as beam steering, molecular quenching, and spectral line broadening are common at high pressures.

An understanding of the complex soot formation processes in combustion systems is required for the study of technical factors associated with sooty combustion which have implications for combustion efficiency and hence, global warming. Therefore, there is a need to develop advanced diagnostic techniques for the very harsh environment of gas turbine combustors burning liquid fuels. This paper presents initial results of an investigation into heavily sooted flames using terahertz (THz) frequency electromagnetic radiation at elevated pressures.

As a relatively new technology, it is worth making a detailed background review. Terahertz waves have a frequency of between 100 and 30 THz (see Fig. 1) which lie between the infrared and microwave parts of the electromagnetic spectrum. This far-infrared, or THz, region is one of the least explored and exploited parts of the electromagnetic spectrum, especially when compared with the relatively well developed science and technology that exists at all other wavelengths. This is because until recently it was very difficult to generate and detect THz radiation efficiently. At present, there is no single electronic device able to oscillate up to frequencies of 1 THz. The current record is set at 700 GHz, produced by resonant tunnelling diodes, but generating very little power (< 10 μW); a review of these latest THz electronic devices can be found in Ref. [1]. Dielectric loss in the

Received October 8, 2008; accepted January 8, 2009

Jason BASSI, Yang ZHANG (✉)
School of Mechanical, Aerospace and Civil Engineering, The University of Manchester, Manchester M13 9PL, United Kingdom
E-mail: yang.zhang@manchester.ac.uk

Mark STRINGER, Bob MILES
School of Electronic and Electrical Engineering, The University of Leeds, Leeds LS2 9JT, United Kingdom

semiconductor substrate is a major limiting factor for generating THz waves in such devices. However, ongoing research suggests that solid state devices will be realized with the potential for portable, low cost, robust and tuneable THz systems.

THz radiation can also be generated by optical techniques, and involves down-conversion using nonlinear processes in electro-optic crystals or semiconductor photoconverters. Currently, the most popular method for generating THz radiation employs femtosecond pulsed lasers (such as Ti-sapphire) and biased semiconductor emitters (commonly GaAs) [2]. This technique produces 10–100 μW of broadband pulsed THz radiation, typically between 0.1–6 THz with 1–2 ps pulse length. Quantum cascade lasers operating at frequencies as low as 2–3 THz and producing >1 mW of power have also been recently demonstrated, but these continuous-wave devices are not tuneable and require cryogenic cooling. Recent developments, made possible by recent progress in THz generation, have demonstrated the potential of THz technology for imaging and spectroscopy in areas ranging from medicine to communications and astronomy [3–8].

Combustion processes have been studied in the wavelength region extending from the ultraviolet region up to the infrared, but now the potential for studies in the relatively unexplored THz spectral region opens new ways to further our understanding of complex multi-phase flow processes. The first THz absorption measurements of a premixed laminar hydrocarbon–air flame have been conducted by Cheville and Grischkowsky using the technique of terahertz time-domain spectroscopy [3,9,10]. They have observed a large number of absorption lines; including those of water, CH and NH_3, establishing the relative abundance of combustion products in this frequency range.

Optical diagnostic laser-based techniques such as laser induced fluorescence (LIF), polarization spectroscopy, CARS and DFWM [11–15] are difficult or impossible to apply in strongly sooted combustion environments, owing to strong absorption, spectral interference from particulate scattering, and fluorescence from large molecules.

The resolution and sensitivity of THz imaging and spectroscopy are still rather limited compared with existing optical and infrared diagnostics. A frequency of one THz corresponds to a wavelength of 300 μm, which is good enough for our purposes because the combustion device is much larger. The initial results presented here show promise for the use of THz radiation sources as a new viable diagnostic tool for the exploration of harsh sooty flame conditions at elevated pressure; where current laser-based methods start to break down.

2 Properties of THz radiation interaction with multi-phase flow

The only fundamental distinction between one spectral region and another is how the electromagnetic radiation interacts with matter. The various bands encompass a broad range of physical processes; radio waves are associated with nuclear magnetic resonance, for example, while gamma rays are produced by decaying or excited atomic nuclei (see Fig. 1).

Terahertz radiation has several key properties which are unique to this part of the electromagnetic spectrum, which has triggered the ever-increasing demand to develop this

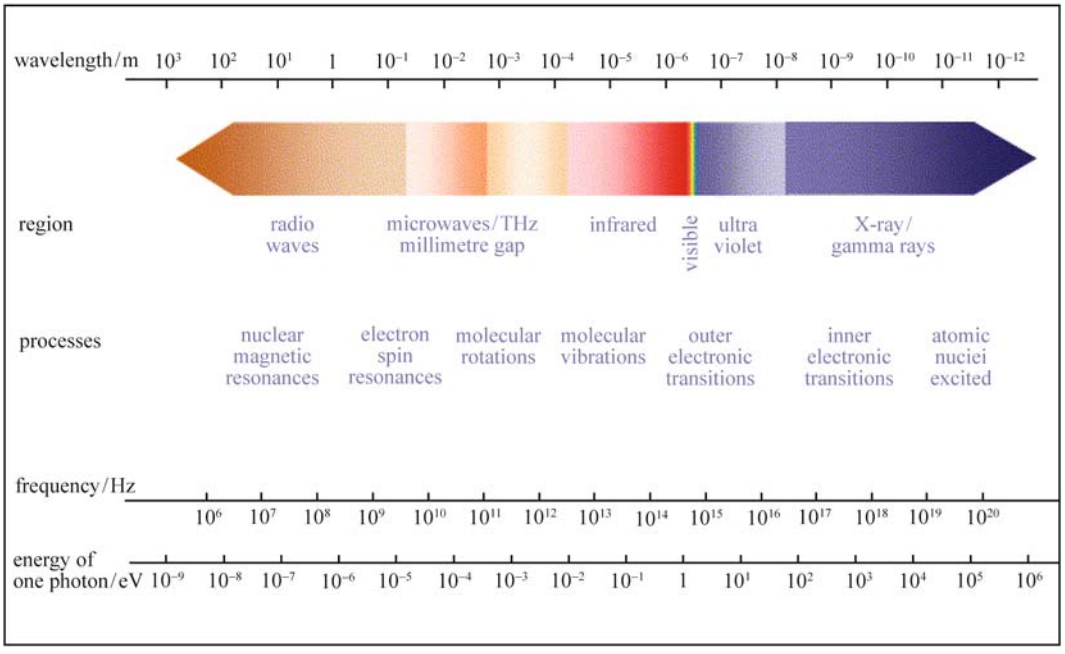

Fig. 1 Electromagnetic spectrum and some of material processes associated with each band

frequency band for many different potential applications. One key property of THz radiation is that it interacts strongly with molecular rotation modes, which exist only in gases. Albert et al. [16] calculated rotational absorption coefficients as a function of radiation frequency and molecular mass, with the results shown in Fig. 2.

The strength of the interaction increases as J_{max} (here the moment of inertia) decreases, which corresponds to a decreasing molecular mass. The interaction strength peaks in the THz region for a wide range of molecules, and is 10^3–10^6 times stronger than interaction strengths in the microwave and infrared bands. This strong coupling to rotation modes is one of the most important features of the THz spectral region.

This characteristic makes the THz region well suited to the study of common combustion species with a small molecular mass, such as CH, OH, H_2O, NO, NH_3, and CO. All these species are currently measured using laser-based diagnostics.

3 Experimental setup

The burner used in this work is based on the design of Miller and Maahs [17] and is contained within a water cooled pressure chamber (with an internal height of 600 mm and an internal diameter of 120 mm) that is capable of continuous operation at pressures up to 1.6 MPa, shown schematically in Fig.3. Classic over-ventilated Burke-Schumman [18] laminar diffusion flame is produced which is stabilized on a nozzle with an exit diameter of 4.57 mm. Ethylene was the selected fuel supplied from a compressed gas cylinder, regulated by a needle valve, and measured by a calibrated mass flow meter with 1% full scale accuracy. The mass flow rates for ethylene were kept constant for all pressures at 0.210 standard liters per minute. Co-flow air is supplied from a compressed air bottle into the burner and is diffused using a layer of glass beads and is followed by a honeycomb structure with 1.5 mm holes which straightens the flow; located 4 mm below the nozzle tip. Nearly uniform co-flow air was achieved with a needle valve and calibrated mass flow meter to produce a constant mass flow rate of 15 standard liters per minute for the ethylene diffusion flame.

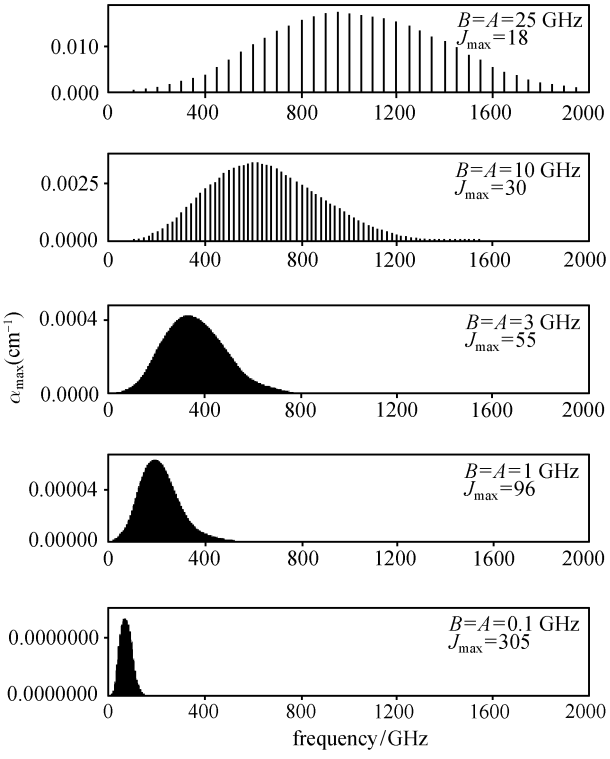

Fig. 2 Rotational interaction strengths in THz region as a function of molecular size (J_{max} is the moment of inertia, which is proportional to the molecular mass) A and B are molecular rotational constants [16]

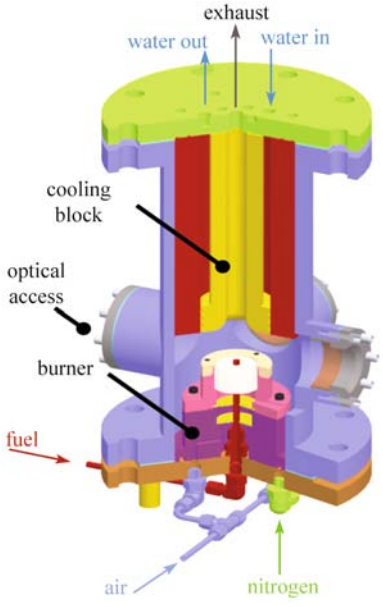

Fig. 3 Cross-section of the high-pressure burner

To pressurize the chamber, nitrogen flow was introduced through the base of the burner using a ring of 1.5 mm holes. The nitrogen flow also keeps the chamber walls cool and the window ports free of condensation and soot. The increase in pressure within the vessel was achieved by increasing the flow rate of nitrogen and simultaneously decreasing the flow rate of the exhaust by adjusting the back-pressure regulating valve which can maintain the chamber pressure anywhere between 0.1 and 1.6 MPa. Optical access to the burner is provided by four windows; two of which are made from fused silica, and two from high-resistivity float-zone silicon (HRFZ-Si), with a diameter of 50 mm and a thickness of 20 mm. The fused quartz windows provide optical access to the visible band

whilst the HRFZ-Si windows provide access to the terahertz band.

A schematic of the THz-TDS setup used in this study is shown in Fig. 4. THz pulses are generated by a Coherent Vitesse 800-2 femtosecond laser. The Vitesse 800-2 is based on an integrated, diode-pumped Nd: YVO4 Verdi laser that generates an average power of 2 W at 532 nm. This beam pumps a mode-locked Ti-sapphire oscillator, which generates pulses of 80 fs duration centered at 800 nm. The repetition rate of the pulsed beam is 82 MHz, and its average power is 300 mW.

As shown in Fig. 4, the 800 nm beam is split after leaving the laser into a pump beam and a probe beam. A 90/10 beam splitter is used for this, with most of the power going to the pump beam. The pump beam is focused on a biased, photoconductive GaAs antenna to generate vertically polarized THz pulses. The THz beam is collimated and focused to a 10 mm diameter beam that is transmitted through the high-pressure burner by a gold-coated parabolic mirror. The optical path of the THz beam is shown in Fig. 4 as a green streak. After the burner, the THz beam passes through a 2 mm thick piece of polyethylene and is then recollimated by a second parabolic mirror. The polyethylene has an absorption coefficient of less than 1 cm^{-1} for frequencies below 4 THz, so it is nearly transparent to the beam [19]. A small, gold-coated, right-angle prism is glued onto the polyethylene plate. This prism is used to combine the THz pulse with the probe beam, which has been delayed and horizontally polarized. The THz beam and probe beam are now collinear, and can be focused onto a 1 mm thick (110)-oriented ZnTe crystal by a second gold-coated parabolic mirror.

The probe beam then passes through a quarter-wave plate and a Wollaston prism. The Wollaston prism separates the probe beam into two orthogonal polarization components, which are subsequently focused onto a balanced photo-diode detector (Nirvana 2017). When no THz electric field is present, both polarization components have the same intensity and the signal from the balanced photo-diode detector is zero. The THz electric field changes the polarization of the probe pulse in the electro-optic crystal from linear to slightly elliptical, thereby inducing a signal that is proportional to the THz electric field. By varying the delay between the probe pulse and the

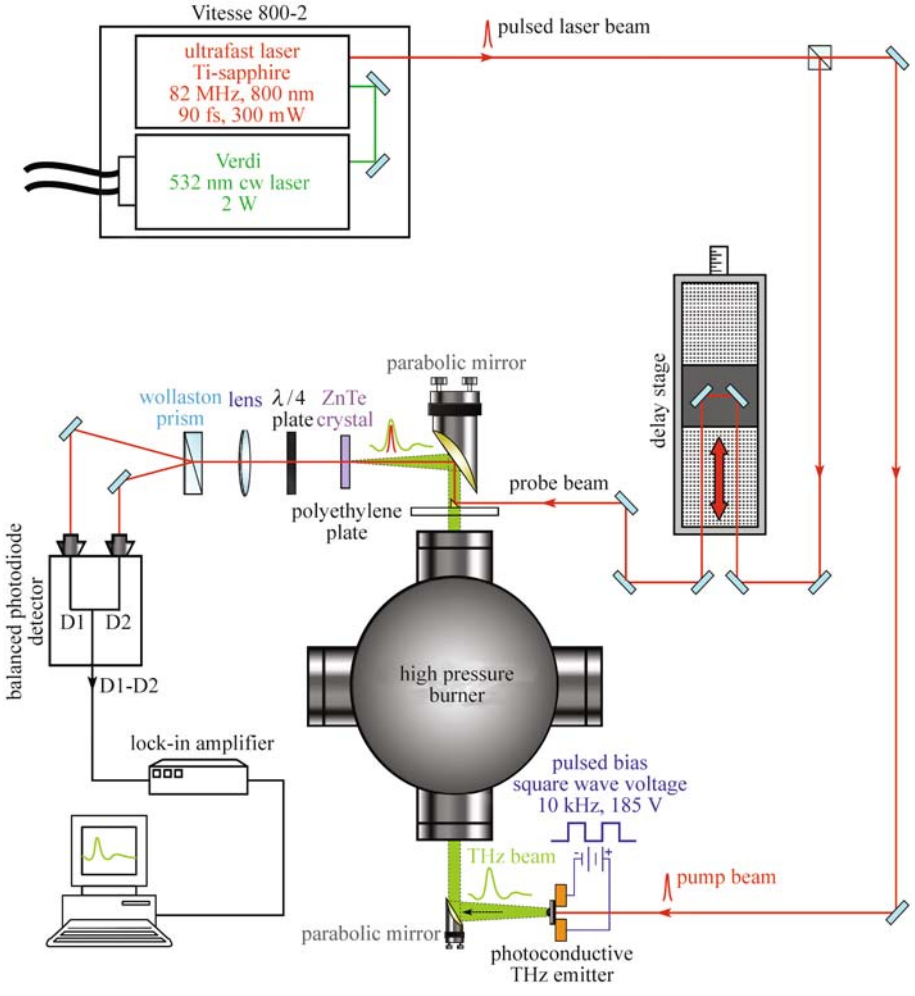

Fig. 4 Schematic of the experimental setup

THz pulse, the complete electric field of the THz pulse can be measured. The time delay is varied by passing the probe beam through a hollow retro-reflector, which is mounted on a mechanical translation delay stage (Melles Griot) with half micron stepper accuracy. Each delay-time scan has a range of approximately 67 ps (10 μm step size) and consists of 2048 different points.

A LabView program with GPIB communications is used to control the translation stage and the lock-in amplifier (which is usually given a time constant of 100 ms) to measure the THz waveforms. The THz spectrum is obtained by applying a fast Fourier transform to the waveform, resulting in a useful bandwidth of 0.2–2.5 THz with a signal-to-noise ratio of 30 dB.

4 Spectral modeling of combustion species in the THz band

This section presents those flame species which have rotational spectral lines in 0.25 THz to 3 THz band. The flame species were identified by consulting the JPL [20] and HITRAN [21] spectroscopic databases. The JPL database contains submillimeter, millimeter, and microwave spectral lines between 0 and 10000 GHz. The information listed for each spectral line includes the frequency, its estimated error, the intensity at 300 K, and the energy and quantum numbers of the lower state. The uncertainty in the line position is different for each line and varies from molecule to molecule, but over the range 0.25–3 THz it typically lies between±0.03 GHz and±0.3 GHz. The JPL catalog was constructed using least-squares fitting to theoretical predictions of the spectral line shapes, which are mostly obtained from the literature. The total absorptions of available combustion species from the JPL database are shown in Fig. 5. These line intensities are given in units of $nm^2 \cdot MHz$, and are based on an integral of the absorption cross-section over the spectral line shape at a temperature of 300 K. It can be seen that water has a large amount of absorption in this bandwidth, and the most intense lines. However, there are windows in the spectrum where CH, OH, and NH_3 transitions are not obscured by the water lines. In the window just above 2.5 THz, for example, CH and OH have intense lines at 2.528 and 2.515 THz respectively.

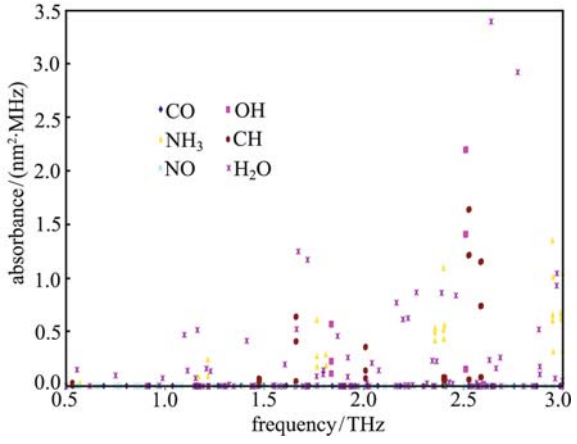

Fig. 5 Spectral lines of combustion species at THz frequencies (integrated absorption)

The HITRAN database contains the same information on spectral line positions, and includes additional information on fundamental molecular parameters (e.g., the dipole moment, partition function, and Lorentz half-width). The complete set of combustion species is tabulated in Table 1. CH is not present in the HITRAN database, but as mentioned before this molecule does have a significant absorption line at 2.528 THz.

Using these molecular parameters, the transmission of a given combustion species at THz frequencies can be predicted and calculated. This task was completed for combustion species in the HITRAN database using the set of algorithms known as LINEPAK [22]. LINEPAK is commonly used in astrophysics research to obtain high-resolution transmission spectra. The absorption spectrum of each molecule (given in terms of the power absorption coefficient, units of cm^{-1}) was calculated for a given temperature, pressure, and peak mole fraction. The peak mole fractions listed in Table 1 for these species refer to a methane diffusion flame, and are taken from Refs. [23,24]. These peak mole fractions may not be strictly correct, since the mole fraction of a species will change along a given path through the flame. The OH fraction is largest in the fuel-lean region of a diffusion flame, for example. In this study, since the absorption spectra are only being compared to obtain their relative orders of magnitude, the use of the peak mole fraction is reasonable.

Table 1 List of combustion species taken from the HITRAN database and their peak mole fractions in a typical methane diffusion flame

combustion species	peak mole fraction	class of molecule
H_2O	0.163	asymmetric top
H_2O_2	~ 1E−5	asymmetric top
HNO_3	~ 1E−5	asymmetric top
HCOOH	~ 1E−5	asymmetric top
NO_2	~ 1E−5	asymmetric top
NH_3	~ 0.008	symmetric rotor
CH_3OH	~ 1E−4	symmetric rotor
CO	0.0335	linear molecule
CH	0.004	linear molecule
OH	0.005	linear molecule
NO	~ 1E−4	linear molecule
HCN	~ 1E−4	linear molecule

Figure 6 presents several calculated absorption spectra of water, at 100 kPa and temperatures of 296, 600, 1200

and 1800 K. The spectra clearly show that water has many absorption lines in the THz band, which is to be expected since it is an asymmetric molecule with three distinct moments of inertia. The complexity (number of lines) of the spectrum increases with increasing temperature. At room temperature, the most prominent absorption lines correspond to rotational states of water in the vibrational ground state (v_2= 0). At the elevated temperature of a diffusion flame, many additional water lines appear which correspond to the next higher vibrational state (v_2= 1) and very high v_2= 0 rotational states. It can also be seen that as the temperature increases, the lines tend to narrow and the overall absorbance drops. This can be attributed to the fact that more of the populated water lines correspond to rotational and vibrational states that lie outside the measurement band. The absorption spectrum at 1200 K agrees very well with that measured by Cheville and Grischkowsky [9] in flame at a temperature of 1150 K. They compared their result with the absorption spectrum of water vapor at room temperature, and found five unidentified lines. They suspected that these were due to methylene CH_2 free radicals, but the absorption spectra in Fig. 6 suggest that these lines are more likely just the higher rotational states of water. It can also be seen that the relative heights of the water lines change with temperature. Thus, the temperature of the water can be calculated by comparing the ratio of two absorption lines at an unknown temperature with the same ratio at a known temperature [4].

Some calculated absorption spectra for water at high temperatures and pressures are shown in Fig. 7. The pressures of 100, 800, and 1600 kPa correspond to temperatures of 1800, 1600, and 1400 K respectively. These values were chosen as representative of the high-pressure flame conditions which were measured using an infrared pyrometer. The water lines become much broader with increasing pressure, even to the point where spectral line positions become difficult to resolve due to collisional broadening effects.

Figure 8 shows the calculated absorption spectra of other

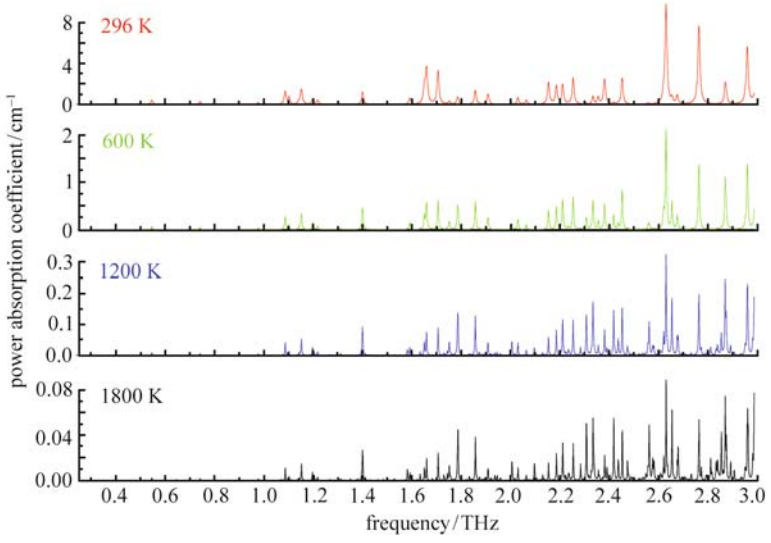

Fig. 6 Calculated absorption spectra of water at 100 kPa and temperatures of 296, 600, 1200 and 1800 K

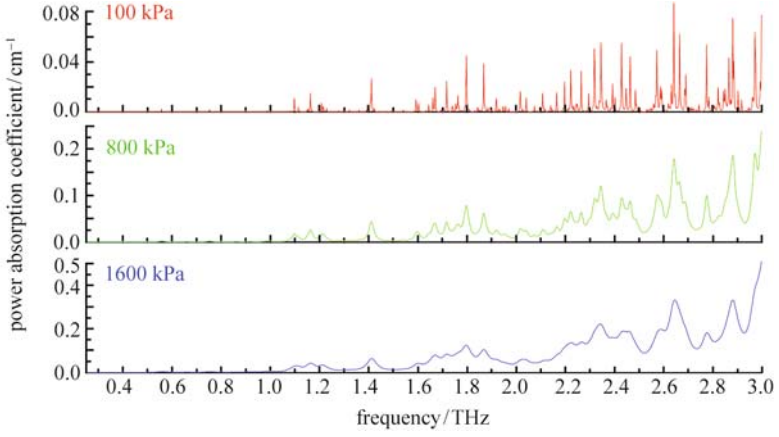

Fig. 7 Calculated absorption spectra of water at 100, 800, and 1600 kPa, and temperatures of 1800, 1600, and 1400 K respectively

combustion species at 100 kPa and 300 K, for the relative peak mole fractions given in Table 1. The linear molecules CO and HCN have very simple spectra: their lines are equally spaced since they only have one distinct moment of inertia. The same can be said of OH, but most of its rotational lines are at frequencies above the THz band used in this study. The large separation of these lines can be related directly to the moment of inertia of the molecule. Comparing the intensity of the diatomic spectra, it can be seen that the absorption lines of CO are 100 orders of magnitude weaker than those of OH even though the peak molar fractions of these two species are very similar. This can be explained by the fact that OH has a dipole moment of 1.67 D (Debye units) which is much larger than CO's dipole moment of 0.112 D. (a zero dipole moment means that there will be no rotation lines.) HCN has a larger dipole moment (2.98 D) than OH, but since its mole fraction is far smaller its intensity of absorption is obviously smaller as well.

The calculated absorption spectra of all discussed combustion species, calculated at a temperature of 296 K, are overlaid for comparison in a logarithmic plot shown in Fig. 9. Water obscures almost all of the other spectral lines, with the exception of four clear windows (marked by arrows in Fig. 8) where NH_3 and OH spectral lines can be seen. These lines are especially evident at 2.51 THz (for OH) and 2.95 THz (for NH_3). It should also be noted that CH and OH have similar mole fractions (see Table 1) so CH should have a slightly less intense line than OH at 2.58 THz (see Fig. 5). Unfortunately, there was not enough information available on CH to run the LINEPAK algorithms. For an elevated temperature of 1800 K (that of a diffusion flame at atmospheric pressure), the full absorption spectrum is shown in Fig. 10. The spectral lines from NH_3 and OH can still be seen, and surprisingly a CO line can also be seen at 2.76 THz (marked with an arrow). HCN, which has a relatively low mole fraction, also has significant peaks at 1800 K. Its absorption intensity is now relatively close to that of water, but the lines are still below the signal-to-noise threshold of a realistic measurement.

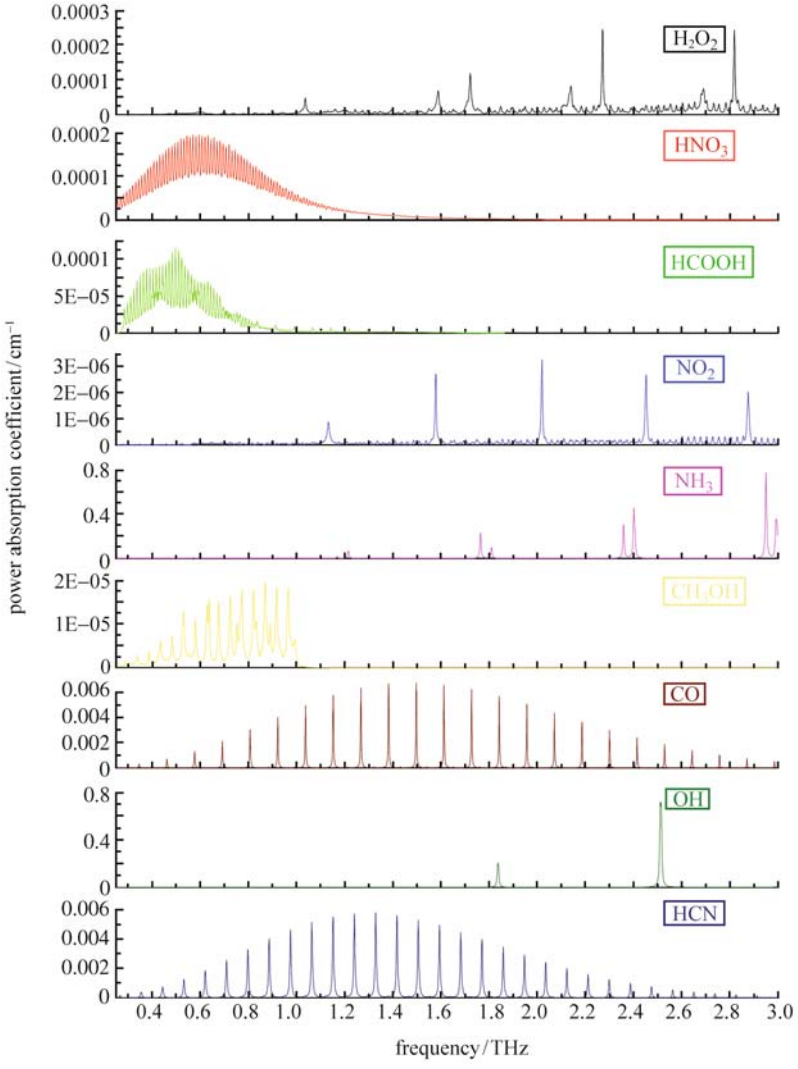

Fig. 8 Calculated absorption spectra of other combustion species at 100 kPa and 300 K

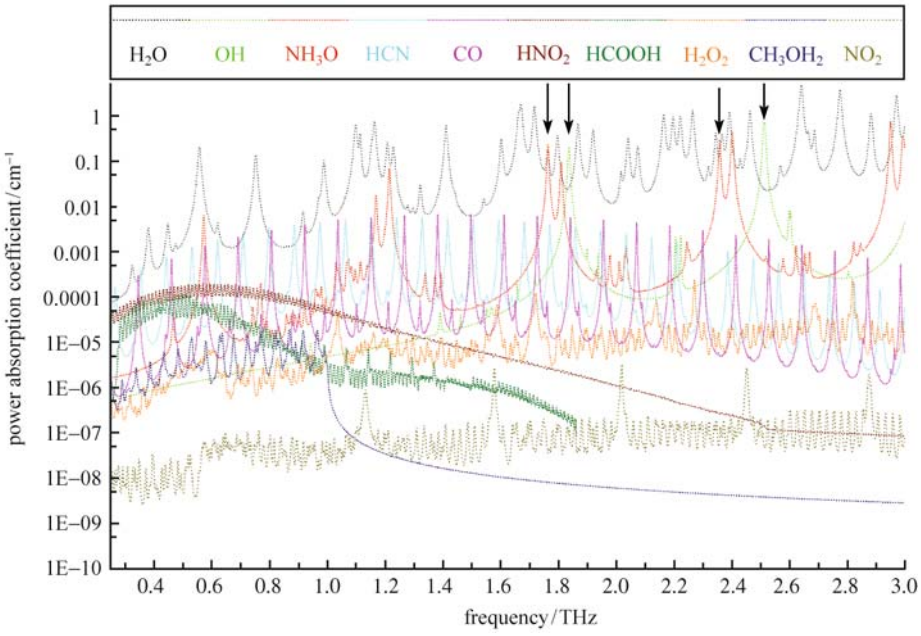

Fig. 9 Calculated absorption spectra of all combustion species at 296 K, log plot

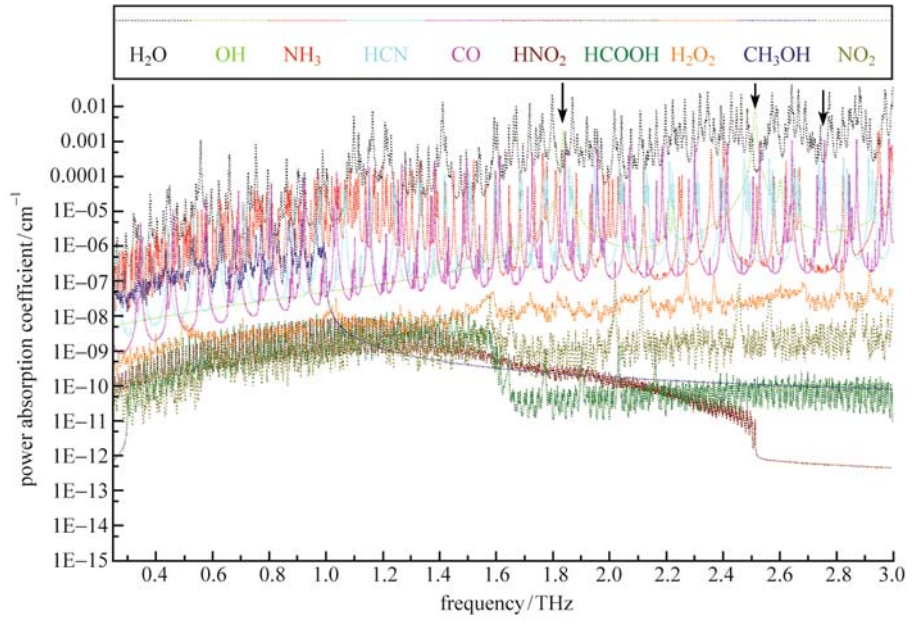

Fig. 10 Calculated absorption spectra of all combustion species at 1800 K, log plot

5 Experimental results

THz-TDS measurements were taken at pressures of 0.1, 0.4, 0.8, 1.2, and 1.6 MPa and the following flow conditions: ethylene and air were supplied to the burner at the constant rates of 0.210 and 15 standard liters per minute respectively for all pressures.

The time domain signals for these pressures are shown in Fig. 11. The weak, rapid oscillations following the pulse contain all the amplitude and phase information related to water absorption. These data make it clear that a time delay is imposed on the THz pulse. Figure 12 shows that there is a perfect linear relationship between time delay and pressure. This time delay is simply due to the increasing refractive index of the denser atmosphere within the burner.

Figure 13 shows the power spectra of THz pulses transmitted through the ethylene flame. The reference

spectrum for atmospheric conditions without a flame is also shown for purposes of comparison. The sharp absorption features which match the water lines calculated in Fig. 7 within 0.005 THz are caused by water. There is no evidence of flame species other than water; even in the window around 2.5 THz where there are no water lines and CH and OH lines should be present. Such small signals, while of great interest, cannot yet be distinguished from the large amount of noise which unfortunately exists at high frequencies.

The amount of absorption occurring within the flame can be calculated by taking the ratio of a flame spectrum to the corresponding reference spectrum. This gives the relative absorption spectra $\alpha(\omega)$:

$$\alpha(\omega) = -\ln\frac{|E_{\mathrm{fl}}|^2}{|E_{\mathrm{ref}}|^2},$$

where, $E_{\mathrm{ref}}(\omega)$ is the reference spectrum, and $E_{\mathrm{fl}}(\omega)$ is the spectrum of the THz beam after propagating through the flame. The absorption transmission spectra of the ethylene flame are shown in Fig. 14. Water absorption features can be seen at all pressures up to frequencies just below 2.5 THz. Beyond this limit, however, the dynamic range of the current THz-TDS setup rapidly approaches unity and the signal is therefore very noisy. The observed decrease in peak signal amplitude with pressure (Fig. 11) is reflected in the absorption transmission spectra in the ethylene flame (Fig. 14), which show a broadband absorption that gradually falls near 2 THz.

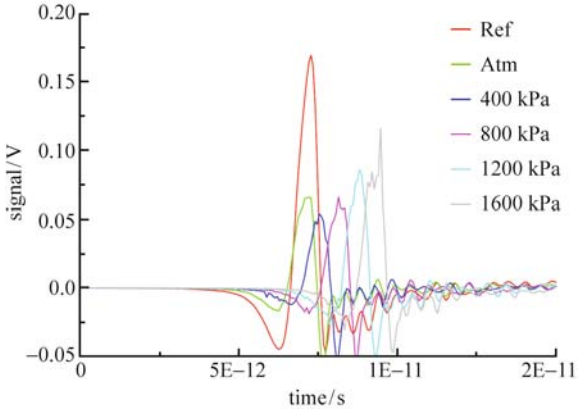

Fig. 11 THz time domain signals at pressures up to 1600 kPa with an ethylene flame, at a constant fuel flow rate of 0.210 standard liters per minute

The power loss (broadband absorption) in the THz signal is most likely due to a distortion of the beam within the flame caused by thermal lensing. Because transverse thermal gradients in the flame create a transverse gradient in the refractive index, the THz beam slightly diverges as it passes through the flame. This change in the beam density is perceived as a drop in transmission.

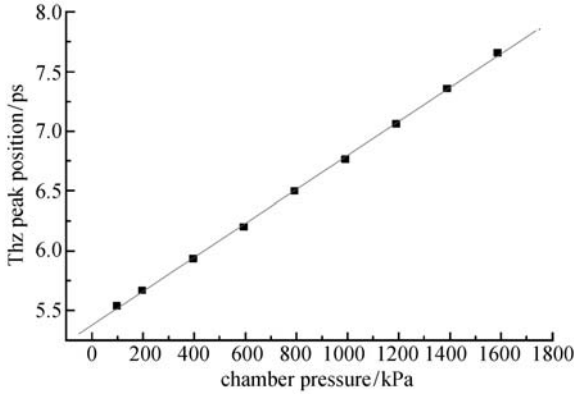

Fig. 12 Plot of THz signal's peak position as a function of chamber pressure

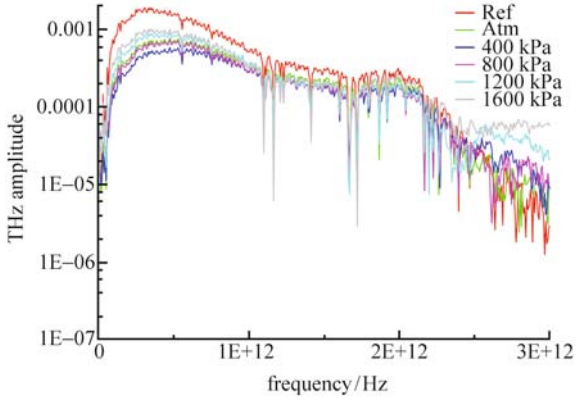

Fig. 13 THz power spectra at pressures up to 1600 kPa with an ethylene flame, at a constant fuel flow rate of 0.210 standard liters per minute

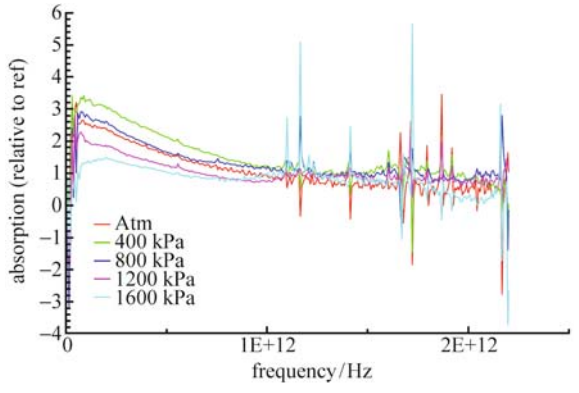

Fig. 14 Relative absorption spectra at pressures up to 1600 kPa of an ethylene flame, at a constant fuel flow rate of 0.210 standard liters per minute

6 Conclusions

Calculations based on the peak mole fractions of these species within a non-premixed flame show that many water lines are present in the bandpass of 0.25 THz to 3 THz. At temperatures approaching that of a non-premixed flame (1800 K) the water lines get weaker, but more lines are also observed from high-order rotational transitions and $v_2 = 1$ vibrational states. At elevated pressures, collisional broadening of the lines should produce a smoother absorption spectrum. Other combustion species are mostly obscured by the many strong water lines, due to their small species/water mole ratio (typically 0.006 %–0.06 %). However, a few windows exist in the bandpass where the water lines are weak. In the numerical model OH and CH lines are observed near 2.5 THz, and NH_3 lines are observed at 1.77 and 2.95 THz. OH has the strongest line, at 2.51 THz. Surprisingly, CO (which has small dipole moment) also produces a very weak but visible feature at 2.76 THz at flame temperature (1800 K).

The experiment in this study has clearly demonstrated that a THz beam can pass through heavily sooted, non-premixed ethylene flame under elevated pressures up to 1.6 MPa. The only lines observed in the THz absorption spectra were from rotational transitions of water in the ground vibrational state. The expected strong OH line at 2.51 THz and slightly weaker CH line at 2.5 THz could not be observed experimentally due to the low dynamic range (~7 at 2.5 THz for flame) of our apparatus at frequencies over 2.5 THz.

Being the first study of its kind, further work is needed with a THz Time-Domain system with a larger dynamic range at THz frequencies greater than 2.5 THz. Systems already exist using a laser with a faster pulse width (i.e., 12 fs) which has a total measurable bandwidth high dynamic range up to 10 THz [25]. Obtaining a dynamic range above 1000 in the 2.5 THz region would enable the observation of the strong OH and CH lines near the 2.5 THz window. Observations of OH, NH_3, and CH would also become far easier, since these lines are much more intense at frequencies greater than 3 THz for the temperatures within a flame. The bandwidth could also be increased by changing the THz emitter from a GaAs crystal to a LT-GaAs crystal. The latter has a shorter free-carrier lifetime of 100 fs, which corresponds to a maximum attainable frequency of 7.5 THz [26].

The THz-TDS technique is developing rapidly, portable electronic devices which produce and detect radiation up to 1 THz (the envelope is constantly being pushed to higher frequencies) are further becoming a reality, and would allow the transition of THz combustion diagnostics from the laboratory to industrial combustion devices.

Acknowledgements This work was supported by EPSRC in the frame of basic technology. Thanks go to Dr W Truscott, the project coordinator, at the University of Manchester.

References

1. Eisele H. High performance InP Gunn devices with 34 mW at 193 GHz. Electronics Letters, 2002, 38 (16): 923–924
2. Nahata A, Weling A S, Heinz T F. A wideband coherent terahertz spectroscopy system using optical rectification and electro-optic sampling. Applied Physics Letters, 1996, 69(16): 2321–2323
3. Cheville R A, Grischkowsky D. Observation of pure rotational absorption spectra in the v_2 band of hot H_2O in flames. Optics Letters, 1998, 23(7): 531–533
4. Cheville R A, Grischkowsky D. Far-infrared foreign and self-broadened rotational linewidths of high-temperature water vapor. Journal of the Optical Society of America B: Optical Physics, 1999, 16(2): 317–322
5. Dykaar D R, Chuang S L. Terahertz electromagnetic pulse generation, physics and applications. Journal of the Optical Society of America B: Optical Physics, 1994, B11(12): 2457–2581
6. Li M, Zhang X C, Sucha, G., et al. Portable THz system and its applications. SPIE Proceedings series, 1999, 3616: 126–135
7. Rønne C, Keiding S R. Low frequency spectroscopy of liquid water using THz-time domain spectroscopy. Journal of Molecular Liquids, 2002, 101(1–3): 199–218
8. Schall M, Helm H, Keiding S R. Far infrared properties of electro-optic crystals measured by THz time-domain spectroscopy. International Journal of Infrared and Millimeter Waves, 1999, 20(4): 595–604
9. Cheville R A, Grischkowsky D. Far-infrared terahertz time-domain spectroscopy of flames. Optics Letters, 1995, 20(15): 1646–1648
10. Cheville R A, Grischkowsky D. Direct observation of the v_2 water rotational band in flames via THz time-domain spectroscopy. Technical Digest–European Quantum Electronics Conference, IEEE, San Francisco, CA, USA, 1998
11. Grisch F, Bouchardy P, Clauss W. CARS thermometry in high pressure rocket combustors. Aerospace Science and Technology, 2003, 7(4): 317–330
12. Joubert P, Bruet X, Bonamy J, et al. H_2 vibrational spectral signatures in binary and ternary mixtures: Theoretical model, simulation and application to CARS thermometry in high pressure flames. Comptes Rendus de l'Academie des Sciences–Series IV: Physics, Astrophysics, 2001, 2(7): 989–1000
13. Bengtsson P-E, Alden M, Kröell S, et al. Vibrational CARS thermometry in sooty flames: Quantitative evaluation of C_2 absorption interference. Combustion and Flame, 1990, 82(2): 199–210
14. Radi P P, Mischler B, Schlegel A, et al. Absolute concentration measurements using DFWM and modeling of OH and S_2 in a fuel-rich H_2/Air/SO_2 flame. Combustion and Flame, 1999, 118(1,2): 301–307
15. Tobai J, Dreier T. Measurement of relaxation times of NH in atmospheric pressure flames using picosecond pump-probe degenerate four-wave mixing, Journal of Molecular Structure, 1999, 480–481: 307–310
16. Albert S, Petkie D T, Bettens R P A, et al. FASSST: A new gas-phase analytical tool. Analytical Chemistry, 1998, 70(21): 719A–727A

17. Miller I M, Maahs H G. High pressure flame system for pollution studies with results for methane-air diffusion flames. Report No. NASA-TN-D-8501 NASA, Langley Research Center, 1977
18. Burke S P, Schumann T E W. Diffusion flames. Ind Eng Chem, 1928, 20(10): 998–100
19. Park H, Cho M, Kim J, et al. Terahertz pulse transmission in plastic photonic crystal fibres. Physics in Medicine and Biology, 2002, 47 (21): 3765–3769
20. Pickett H M, Poynter R L, Cohen E A, et al. Submillimeter, millimeter, and microwave spectral line catalog. Journal of Quantitative Spectroscopy and Radiative Transfer, 1998, 60(5): 883–890
21. Rothman L S, Jacquemart D, Barbe A, et al. The HITRAN 2004 molecular spectroscopic database, Journal of Quantitative Spectroscopy and Radiative Transfer, 2005, 96(2 Spec. Iss.): 139–204
22. Gordley L L, Marshall B T, Chu D A. Linepak: algorithms for modeling spectral transmittance and radiance, Journal of Quantitative Spectroscopy and Radiative Transfer, 1994, 52(5): 563–580
23. Ju Y, Niioka T. Computation of NOx emission of a methane-air diffusion flame in a two-dimensional laminar jet with detailed chemistry. Combustion Theory and Modelling, 1997, 1(3): 243–258
24. Kaplan C R, Patnaik G, Kailasanath K. Universal relationships in sooting methane-air diffusion flames. Combustion Science and Technology, 1998,131(1–6): 39–65
25. Kono S, Tani M, Gu P, Sakai K. Detection of up to 20 THz with a low-temperature-grown GaAs photoconductive antenna gated with 15 fs light pulses. Applied Physics Letters, 2000, 77(25): 4104–4106
26. Duvillaret L, Garet F, Roux J F, et al. Analytical modeling and optimization of terahertz time-domain spectroscopy experiments using photoswitches as antennas. IEEE Journal on Selected Topics in Quantum Electronics, 2001, 7(4): 615–623